Uncertainty propagation and sensitivity analysis for a better understanding of the flow excursion instability with the system code CATHARE

Alberto Ghione

Uncertainty propagation and sensitivity analysis for a better understanding of the flow excursion instability with the system code CATHARE

A. Ghione
Université Paris-Saclay, CEA, Service de Thermohydraulique et de Mécanique des Fluides, 91191, Gif-sur-Yvette, France
alberto.ghione@cea.fr

ABSTRACT

The flow excursion (or Ledinegg) instability is a limiting safety issue in research reactors, since it may lead to boiling crisis in some of the core channels. Reliable and precise simulations of this phenomenon are therefore essential. The thermal-hydraulic system code CATHARE is used for safety analysis studies, and was validated against flow excursion experiments proving good performances. In order to obtain a better understanding of the code behavior, an uncertainty propagation and sensitivity analysis was carried out.
The study focuses on the simulation of a Whittle-Forgan flow excursion experiment, performed in a uniformly heated vertical narrow rectangular channel at low pressure. The input uncertain parameters associated to the geometry, the initial and boundary conditions and CATHARE closure laws were identified and quantified in terms of *pdf*s. An uncertainty propagation was then carried out. The obtained 95%-95% tolerance interval of the mass flow-rate predicted at flow excursion is relatively large (relative variations compared to the nominal flow-rate up to 30%) indicating a significant impact of the uncertainties on flow excursion simulations in CATHARE.
Using the same set of calculations, a sensitivity analysis is performed to determine the most influential input parameters, computing the Pearson and Spearman sensitivity coefficients. The result shows that the uncertainties on the sub-cooled condensation CATHARE model and on the gap size have the largest impact.
These results are compared to the ones obtained with the Sobol methodology, which gives a more reliable and complete sensitivity analysis, but more expensive in terms of number of calculations. Similar and consistent outcomes are obtained for this specific application.

KEYWORDS
Flow Excursion Instability, Uncertainty propagation, Sensitivity analysis, CATHARE, Research Reactor

1. INTRODUCTION

Nuclear research reactors are essential to support commercial nuclear power plants, develop new fuels and materials for future reactors, and produce radioisotopes for medical applications. In the core of these reactors, the water usually flows at relatively low pressure (< 1 MPa) in narrow channels that are positioned in a parallel configuration (no cross flows). This design allows to remove huge quantities of heat within a compact volume. The parallel arrangement may cause the so-called flow excursion instability (or Ledinegg instability [1, 2]). This phenomenon is generated by the uneven distributions of power and flow in the core, which may lead to the redistribution of the flow from the hottest channels to the colder ones. As a consequence, the hottest channels are deprived of the coolant, eventually leading to the boiling crisis and a sudden increase of the cladding and fuel temperatures.
The prediction of this phenomenon is therefore of crucial importance for the design studies and the safety analyses of research reactors. In France, the Best-Estimate (BE) thermal-hydraulic system code CATHARE [3] is used. It has been developed by the French Alternative Energies and Atomic Energy Commission (CEA), the French utility EdF, the reactor vendor Framatome and the French Nuclear

Safety Institute (IRSN). The code has been extensively validated for conditions that are representative of pressurized water reactors and, more recently, its validation has been extended to research reactors [4-7].
In this paper, an uncertainty and sensitivity analysis of a Whittle-Forgan flow excursion experiment [8] was carried out using the statistical platform URANIE [9]. This study allows a better understanding of the code CATHARE behavior when simulating the flow excursion instability and the most influential parameters can be determined.

The paper is organized as follows: Section 2 briefly introduces the flow excursion instability; Section 3 presents the methodologies for the uncertainty and sensitivity analysis; Section 4 describes the Whittle-Forgan experiment; in Section 5, the results are shown and discussed; in Section 6, conclusions are drawn.

2. FLOW EXCURSION INSTABILITY

The prediction of the flow excursion instability [1, 2] is one of the most important safety criteria in research reactors, since it may cause the boiling crisis in the hottest core channels. The Onset of Flow Instability (OFI) occurs when the slope of the pressure drop - mass flux curve for the external supply system (e.g., imposed by a pump characteristic) becomes larger than the one for the internal channel demand:

$$\left.\frac{\partial \Delta p}{\partial G}\right|_{Supply} \geq \left.\frac{\partial \Delta p}{\partial G}\right|_{Demand} \quad (1)$$

The OFI mechanism is schematically represented in Figure 1. The typical demand curve of a heated channel (also called S- or flow redistribution curve) is indicated by the blue line. The system of parallel channels in the core imposes an approximately constant total pressure drop. Thus, the supply curve is horizontal (red line). The operating conditions corresponds to the intersection between the two curves.

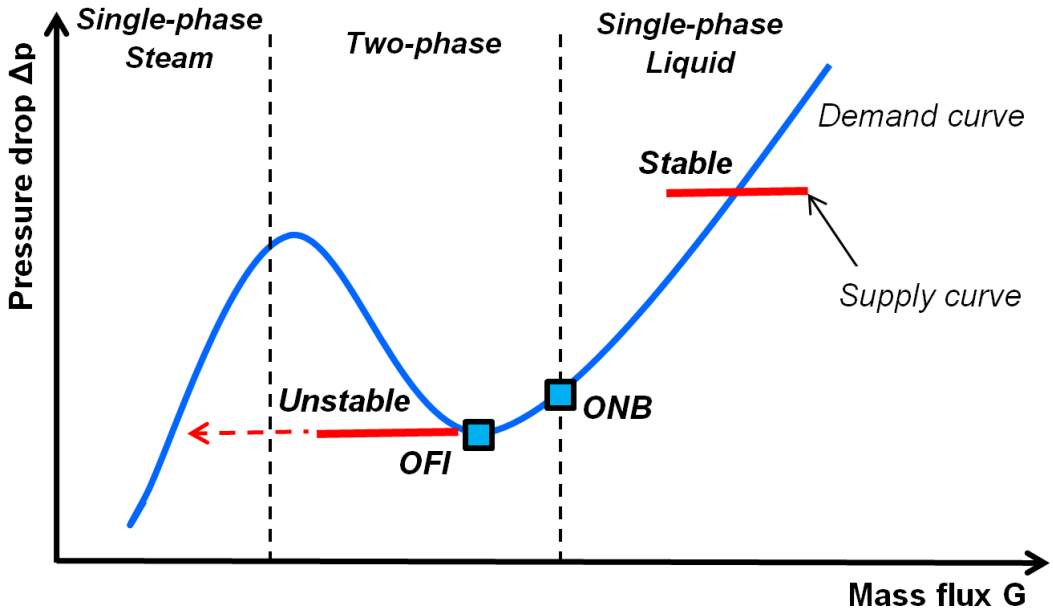

Figure 1. Onset of Flow Instability for heated parallel channels.

In the single-phase liquid region, the mass flux is sufficiently high and the system is stable, since the slope of the supply curve is smaller than the one of the demand curve. If the mass flux decreases at constant heat flux, the pressure drop in the heated channel decreases. Eventually, the Onset of Nucleate Boiling (ONB) is reached. Small bubbles are then generated at the heated walls, but the slope of the demand curve remains positive due to the negligible void fraction. The operating point is still stable.

For lower mass fluxes, the steam bubbles grow and they begin to detach from the walls. The void fraction starts to increase significantly. This phenomenon is usually called Onset of Significant Void (OSV) or Net Vapor Generation (NVG). The growing void fraction in the channel leads to a progressive decrease of the slope of the S-curve, until the minimum of the demand curve (zero slope) is reached. Since the slope of the supply curve is also zero, then the OFI coincides with this minimum. Therefore, the NVG anticipates the OFI [6]. This is due to the fact that, although a fast growth of void fraction begins from the NVG point, a large part of the channel remains in single-phase conditions.

At the OFI point, a further decrease of the mass flux causes a sudden flow redistribution transient. The system enters in an unstable operating region where the void fraction rapidly grows. The associated increase of the channel resistance causes a further reduction of the mass flow rate and therefore an enhancement of the void production (positive feedback). Eventually, the channel operates in the pure single-phase steam region. This operating point is again stable since the slope of the S-curve is positive. The flow excursion instability can thus trigger the occurrence of the critical heat flux.

In this paragraph, the OFI mechanism have been explained via a transient reducing the mass flux with all other parameters kept constant. However, the OFI conditions may be also achieved through other transients, e.g. increasing the heat flux to one of the parallel channels.

3. METHODOLOGY

In this chapter, the statistical tools used for the propagation of uncertainties and the sensitivity analysis are briefly presented.

3.1. Propagation of input uncertainties

In order to study the impact of the uncertainties on the CATHARE simulations, the GRS methodology [10] for the propagation of input errors is used in this article. The uncertainties associated to the geometry of the system, the initial and boundary conditions, and the relevant physical models of the code are identified and quantified in terms of probability distribution functions (*pdf*s). The determination of these pdfs relies on different sources, such as specifications from the manufacturers, appropriate experiments and the literature. If data are not sufficient or available, then expert judgment is employed.

A Simple Random Sampling (SRS) is used to generate samples of the input uncertainties. These samples are used to perform CATHARE simulations where all the uncertain parameters are varied simultaneously. From the statistical analysis of the code results, uncertainty bands for the output Quantities of Interest (QoIs) can be quantified.

The number of required simulations N, equal to the size of input samples, is determined by the desired tolerance interval for the output QoIs. A tolerance interval is defined as an interval that includes at least a portion q of the population under study, with a confidence level γ. The Wilks' formula [7, 11] can be employed:

$$\gamma \geq 1 - \sum_{s=0}^{r+m-1} \binom{N}{s} (1-q)^s q^{N-s} \tag{2}$$

This equation permits to estimate N in such a way that at least a portion q of the population lies between the r^{th} smallest and the m^{th} largest value of the sample, with a confidence level γ. The use of r and m larger than one allows a more precise estimation and improves the associated sensitivity analysis [12]. For safety studies, the regulatory authorities usually accept value for q and γ equal to 0.95. The number of code runs necessary in such a case is reported in Table 1. In this study, the size of the samples was chosen equal to 336, which corresponds to $r + m$ equal to 11.

Table 1. Minimum number of code runs with q and γ equal to 0.95, according to Eqn. (2).

$r+m$	N	$r+m$	N	$r+m$	N	$r+m$	N
1	59	**4**	153	**7**	234	**10**	311
2	93	**5**	181	**8**	260	**11**	336
3	124	**6**	208	**9**	286	**12**	361

3.2. Sensitivity analysis

In order to assess the influence of the input parameters on the output QoIs, a sensitivity analysis can be performed. This analysis can also help us to better understand the importance of the different physical models/phenomena on the flow excursion and to identify which modelling improvements are possibly necessary. Three sensitivity indicators are employed in this article: the Pearson correlation coefficients, the Spearman correlation coefficients, and the Sobol sensitivity indexes.

3.2.1. Correlation coefficients: Pearson and Spearman

The Pearson and Spearman correlation coefficients are used to study the correlation between an input and an output of a code. They can be calculated comparing the input and output samples generated during the propagation of uncertainties (subsection 3.1). Their values range between -1 and +1. A value larger than zero corresponds to a positive correlation, i.e. an increase of the input determines an increase in output. Conversely, a value smaller than zero indicates a negative correlation, i.e. the output decreases with an increase of the input. A zero value implies no correlation. The larger the absolute value of the sensitivity coefficients, the stronger the relationship between input and output is. A critical value of the absolute correlation coefficients is often defined to identify when the contribution of the input parameter is significant to the output variability. In this analysis, the chosen critical value is equal to 0.2, so that the significance level (i.e. the probability to reject the true hypothesis that two parameters are not correlated) can be very low, i.e. about 0.00023 for a two-tailed test [13,14].

The Pearson correlation coefficient quantifies the linear relationship between two sets of data. It is computed as the ratio between the covariance of the two samples and the product of their standard deviations [15]. For an output y and input parameter x_i, the coefficient reads:

$$c_{Pearson,i} = \frac{\sum_{k=1}^{N}(x_{i,k}-\bar{x_i})(y_k-\bar{y})}{\left(\sum_{k=1}^{N}(x_{i,k}-\bar{x_i})^2 \sum_{k=1}^{N}(y_k-\bar{y})^2\right)^{1/2}} \quad (3)$$

where $x_{i,k}$ and y_k are the k^{th} components of the two sets; and $\bar{x_i}$ and $\bar{y}$ are the mean values.

The Spearman rank correlation coefficient uses a non-parametric approach, based on the ordered ranks of the sample values (indicated as r_y and r_{xi}). Thus, the coefficient measures the monotonic relationship between the two samples [15]. Similarly to the Pearson coefficient, the Spearman correlation is computed as the ratio between the covariance of the ranked samples and the associated standard deviations:

$$c_{Spearman,i} = \frac{cov\ (r_y, r_{xi})}{std(r_y)\ std(r_{xi})} \quad (4)$$

3.2.2. Sobol sensitivity indexes

The variance-based sensitivity analysis relies on the work of Sobol [16]. The variance of the code output y is decomposed into fractions, which can be attributed to the different input parameter x_i (I is the total number of inputs):

$$Var(y) = \sum_{i=1}^{I}\sigma_i^2 + \sum_{i<k}^{I}\sigma_{ik}^2 + \sum_{i<k<w}^{I}\sigma_{ikw}^2 + \cdots + \sigma_{12\ldots I}^2 \quad (5)$$

The conditional variances are defined as: $\sigma_i^2 = Var[E(y|x_i)]$; $\sigma_{ik}^2 = Var[E(y|x_i x_k)] - \sigma_i^2 - \sigma_k^2$ and so on. Based on this decomposition, the Sobol sensitivity indexes read:

$$S_i = \frac{\sigma_i^2}{Var(y)} \quad ; \quad S_{ik} = \frac{\sigma_{ik}^2}{Var(y)} \quad ; \quad \dots \tag{6}$$

These indexes can vary between 0 and 1 and their sum is equal to 1. They can be interpreted in terms of percentage of the output variance explained by the different input parameters (First-order indexes S_i) and their interactions (Higher-order indexes: $S_{ik} \dots S_{1,2,\dots,I}$). A total number of $(2^I - 1)$ indexes can be therefore computed. In order to reduce the number of indexes, the associated computational cost and simplify their interpretation, Homma and Saltelli [17] introduced the Total-effect sensitivity index to evaluate the global impact of one input parameter on the output variance (i.e. the individual impact plus the impact of its parametric interactions):

$$S_{Ti} = S_i + \sum_{i \neq k} S_{ik} + \sum_{i \neq k \neq w, k<w} S_{ikw} + \cdots \tag{7}$$

In practical applications, when the number of input parameters I is high, only the first-order and the total-effect sensitivity indexes are usually computed. In this case, the number of necessary simulations is equal to $n \cdot (I + 2)$, where n is the Monte Carlo sample size chosen by the user. The number of simulations determines the quality of the estimation of the Sobol indexes. In order to measure this quality, the 95% confidence intervals of the Sobol index estimators are computed using the Martinez methodology [18]:

- For the First-order indexes:

$$\left[\tanh\left(\frac{1}{2}\ln\left(\frac{1+S_i}{1-S_i}\right) - \frac{1.96}{\sqrt{n-3}}\right); \quad \tanh\left(\frac{1}{2}\ln\left(\frac{1+S_i}{1-S_i}\right) + \frac{1.96}{\sqrt{n-3}}\right) \quad \right] \tag{8}$$

- For the Total-effect indexes:

$$\left[1 - \tanh\left(\frac{1}{2}\ln\left(\frac{2-S_{Ti}}{S_{Ti}}\right) + \frac{1.96}{\sqrt{n-3}}\right); \quad 1 - \tanh\left(\frac{1}{2}\ln\left(\frac{2-S_{Ti}}{S_{Ti}}\right) - \frac{1.96}{\sqrt{n-3}}\right) \quad \right] \tag{9}$$

The higher the number of simulations, the higher is the quality of the results (i.e. smaller confidence intervals).

If the relationship between the output and the input parameters is linear, the higher order indexes are equal to zero, the first order indexes are equal to the total ones and their sum is equal to one. In this case, the first order indexes are equal to the square of the Pearson coefficients.

4. WHITTLE-FORGAN EXPERIMENT

The Whittle-Forgan experiments [8] consist of 66 flow excursion tests performed in vertical narrow rectangular channels at low pressure (< 1.7 bar). The current study focuses on the simulation of one of those tests with gap size of 3.23 mm and upward flow of demineralized water.

4.1. Test section

The test section consists of a single vertical narrow rectangular channel that is electrically heated. A schematic representation of its cross sectional area is shown in Figure 2. The geometric features of the test section are reported in Table 2. An axially uniform heat flux profile is generated via direct electrical heating in the heated plates, while the short sides of the lateral corners are mostly un-heated.

Table 2. Test section geometry.

Gap [mm]	l_{heat} [mm]	L_{heat} [mm]	D_{hydr} [mm]	L_{heat}/D_{heat}
3.23	25.4	609.6	5.72	94.5

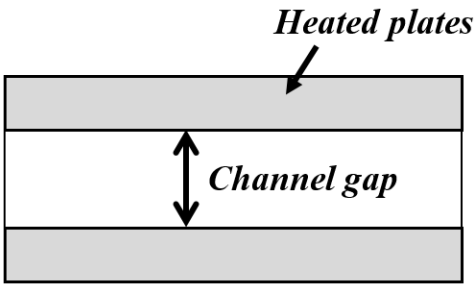

Figure 2. Schematic representations of the test section (top view).

4.2. Test procedure and range of condition

The minimum of the flow redistribution curve (i.e. the OFI) was determined experimentally reducing step by step the mass flux, while keeping constant the inlet temperature, the outlet pressure and the power to the heated plates. For each step, the quantities of interest (i.e. the total pressure drop and the mass flux) were measured in steady-state conditions. The pressure taps used to measure the total pressure drop were placed in adiabatic zones, at the bottom and at the top of the test section. These adiabatic zones connect the test section to the rest of the cooling circuit. Only the minimum of the S-curve are reported by Whittle-Forgan.

The experimental conditions for the analyzed test are: heat flux (ϕ) of 1.04 MW/m^2; outlet pressure (p_{out}) of 1.17 bar; inlet temperature (T_{in}) of 55 °C. The experimental mass flux at OFI is equal to 2356.5 kg/m^2/s.

Several uncertainties (e.g. due to the thermal deformations of the test section, on the pressure and mass flowrate measurements, on the identification of the OFI conditions) may influence the experimental results. These input uncertainties are not known, thus the uncertainty on the experimental results could not be quantified.

4.3. CATHARE modelling of the experiment

The experimental procedure is simulated with CATHARE. The mass flowrate is decreased until the minimum of the S-curve is calculated. The decrease of the flowrate is slow and continuous.

As shown in Figure 3, the test section is modeled as a 1-D channel using the hydraulic diameter presented in Table 2. The heated length is discretized with 140 meshes so that the center of the computational cells coincide with the position of the experimental measurements. The results are proven to be mesh independent. The respect of the global heat balance is verified comparing the experimental and computed outlet liquid temperature.

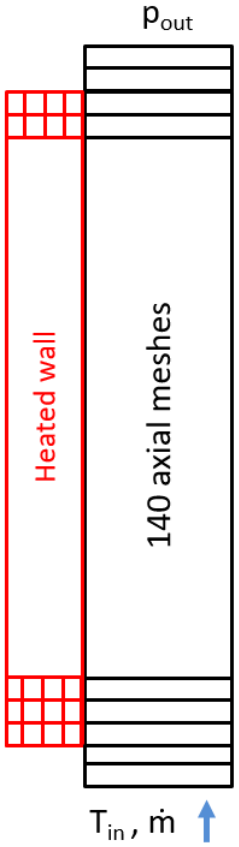

Figure 3. CATHARE nodalisation.

3. RESULTS AND DISCUSSION

In this chapter, the results of the uncertainty propagation and of the sensitivity analysis are presented and discussed. After identification and quantification of the uncertain input parameters (Section 5.1), a propagation of uncertainties is performed to statistically define the 95% / 95% confidence interval of

the output quantity of interest, i.e. the mass flux at the minimum of the S-curve (Section 5.2). The objective is to evaluate the impact of the input uncertainties on the flow redistribution phenomenon. The most influential input uncertainties are then determined via the sensitivity analysis (Section 5.3). Using the simulations from the uncertainty propagation, the Pearson and Spearman correlation coefficients are computed. These sensitivity measures are compared to the Sobol indexes which gives a more complete and reliable sensitivity analysis, but more computationally expensive.

5.1. Identification and quantification of relevant input uncertainties

The first step for the uncertainty and sensitivity analysis is to identify the input uncertainties and quantify them in terms of probability distribution functions. A list of uncertainties with their *pdf*s was compiled. A summary is reported in Table 3.

Table 3. Selected input uncertainties: range and distributions (EJ = Expert Judgement).

Parameter	Distribution	Range	Reference
CATHARE closure laws			
Subcooled condensation (SP1QLE)	Log-uniform	[0.3, 3.0]	[19]
Single-Phase friction factor (SP1CL)	Normal	[0.92, 1.08]	[5]
Two-phase friction multiplier (P1CLGN)	Uniform	[0.8, 1.2]	[19]
Interfacial friction (SP1TOI)	Log-normal	[0.4, 2.2]	[20]
NVG point (P1NVGP)	Normal	[0.85, 1.15]	[20]
Wall heat transfer in nucleate boiling (PCNB)	Normal	[0.56, 1.44]	[21, 22]
Wall heat transfer in turbulent forced convection (PCFLT)	Log-normal	[0.5, 2.0]	[20]
Wall heat transfer in laminar forced convection (PCFLL)	Log-normal	[0.5, 2.0]	[20]
Wall heat transfer in turbulent natural convection (PCNLT)	Log-normal	[0.5, 2.0]	[20]
Wall heat transfer in laminar natural convection (PCNLL)	Log-normal	[0.5, 2.0]	[20]
Geometry, initial and boundary conditions			
Gap	Uniform	± 10 %	EJ
Inlet temperature (T_{in})	Uniform	± 1.0 °C	EJ
Heat flux (ϕ)	Uniform	± 1.5 %	EJ
Outlet pressure (p_{out})	Uniform	± 1.0 %	EJ

The uncertain input parameters are supposed to be independent. The uncertainties on the geometry, the initial and boundary conditions are determined via expert judgement. The uncertainties associated to the CATHARE closure laws relies on a literature review of previous works at CEA. Those uncertainties are applied to the closure laws using multiplicative factors. For example, the single-phase friction factor f is modified with the multiplicative factor SP1CL as:

$$f_{mod} = SP1CL \cdot f \tag{10}$$

5.2. Propagation of input uncertainties

The minimum of the flow redistribution curve corresponds to the OFI condition in a parallel channel configuration. The experimental mass flux at such a minimum is compared to the value obtained by the

BE simulation with CATHARE for the selected test. The relative difference is less than 0.6 %. The code can therefore reproduce the flow excursion phenomenon in a fully satisfactory way, as also shown in Figure 4 and Table 4. In the figure, the red curve is the BE (or nominal) simulation, the blue curves represents the 336 S-curves computed during the uncertainty propagation and the black vertical line indicates the experimental mass flux at OFI.

The propagation of uncertainties was performed sampling the input parameters of Table 3 with a SRS technique. The size of the samples was chosen equal to 336. As discussed in Section 3, all the uncertain parameters were varied simultaneously for each of the calculations. The CATHARE input files were automatically modified and executed by URANIE. All the performed simulations were successful, so that no treatment of the failed runs was necessary. The 336 calculations allow to estimate the tolerance limits with $r + m = 11$, given q and γ equal to 95 % (see Table 2).

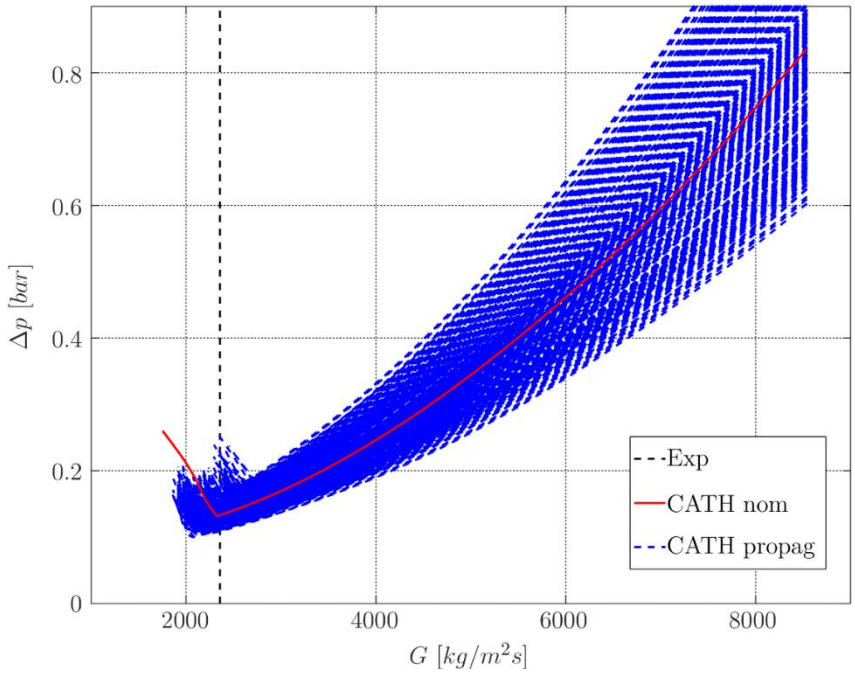

Figure 4. Flow excursion curve: propagation of input uncertainties.

The 95% - 95% confidence interval and the minimum and maximum values of the mass flux at OFI are reported in Table 4. The confidence interval is symmetric around the BE value and relatively large (relative difference between - 20% and + 30%). This indicates that the minimum of the S-curve is particularly sensible to the selected input uncertainties.

Table 4: Mass fluxes at the minimum of the flow excursion curve.

Experimental	BE value	95% - 95% confidence interval	Min – Max
2356.5	2343.3	1921.1 – 2832.3	1872.0 – 2936.4

5.3. Sensitivity analysis

The most influential input uncertainties are determined via the sensitivity analysis.

5.3.1. Pearson and Spearman correlation coefficients

Using the set of CATHARE calculations provided by the uncertainty propagation, the Pearson and Spearman correlation coefficients are evaluated between the uncertain input parameters and the output quantity of interest. As discussed in subsection 3.2.1, a critical value equal to 0.2 is used to determine if

a correlation exists with a significance level below 5 %. The results of the sensitivity analysis is shown in Figure 5.

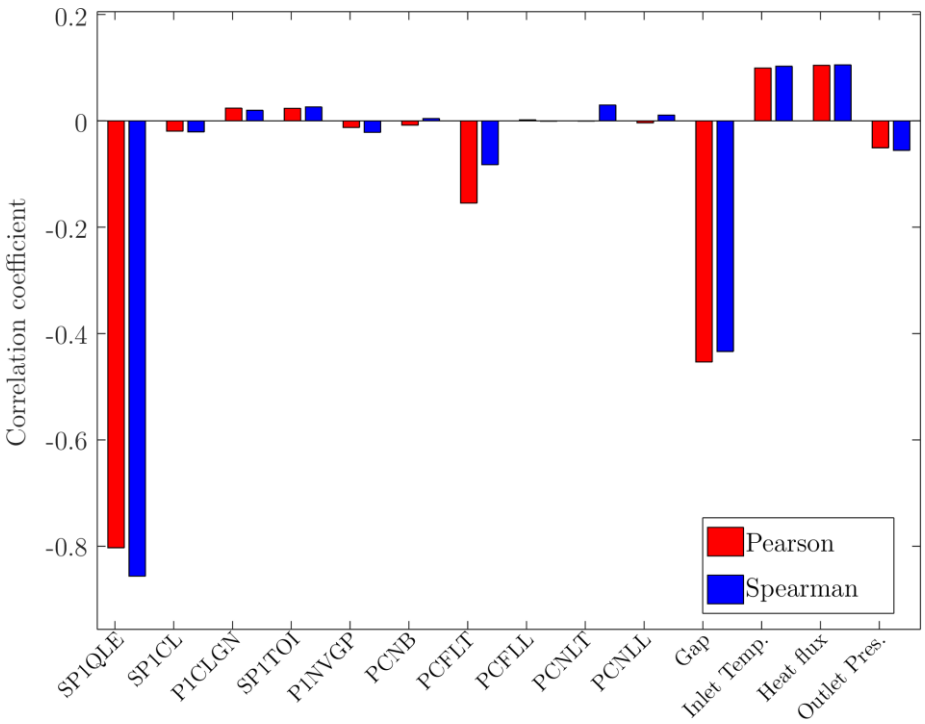

Figure 5. Correlation coefficients.

The most influential parameters are: SP1QLE, which modifies the sub-cooled condensation model in CATHARE, and the gap size between the heating plates. The associated correlation coefficients are negative, i.e. an increase of SP1QLE or of the gap determines a decrease of the mass flux at OFI (or vice versa). The sub-cooled condensation model affects the formation of void fraction in the channel. Enhancing the condensation leads to a reduction of the void fraction, which reduces the pressure drop in the channel and therefore delays the occurrence of the S-curve minimum. Analogously, the gap size influences the pressure drop in the channel, and consequently the OFI point. Both the Pearson and the Spearman coefficients give a similar outcome indicating that the correlation is mainly linear (the sum of the Pearson coefficients squared is equal to 0.9). The other parameters have a secondary influence.

5.3.2. Sobol sensitivity analysis

The Sobol methodology produces a more complete and reliable sensitivity analysis, but more computationally expensive. In order to compute the first-order and the total-effect indexes, $n \cdot (I + 2)$ simulations are needed. Since the number of uncertain input parameters I is 14 and n is chosen equal to 1000, a total number of 16000 CATHARE simulations was performed.

The results of the analysis are shown in Figure 6 and reported in Table 5. The SP1QLE parameter is the most influent and explains approximately 73% of the output variance. The gap size has a significant importance and explains 22 % of the output variance. These two contributions can explain most of the output variance (i.e. 95 %), and the other parameters are negligible. The total-effect sensitivity indexes are almost identical to the corresponding first-order ones. This indicates that there are no significant interactions between the input parameters. Therefore, the output quantity of interest can be expressed as a linear additive function of the SP1QLE parameter and the gap. Due to this linear dependence, the Sobol analysis leads to conclusions that are consistent with the ones obtained using the Pearson and Spearman coefficients (Section 5.3.1).

It is interesting to observe that the first-order indexes are slightly higher than the total ones. This can be

explained considering that the first-order indexes are estimated with less precision than the total ones, especially when the indexes are close to zero (compare the confidence intervals in Table 5). To reduce this inconsistency, an improvement of the estimation quality would be necessary, for example, increasing significantly the Monte Carlo sample size *n*.

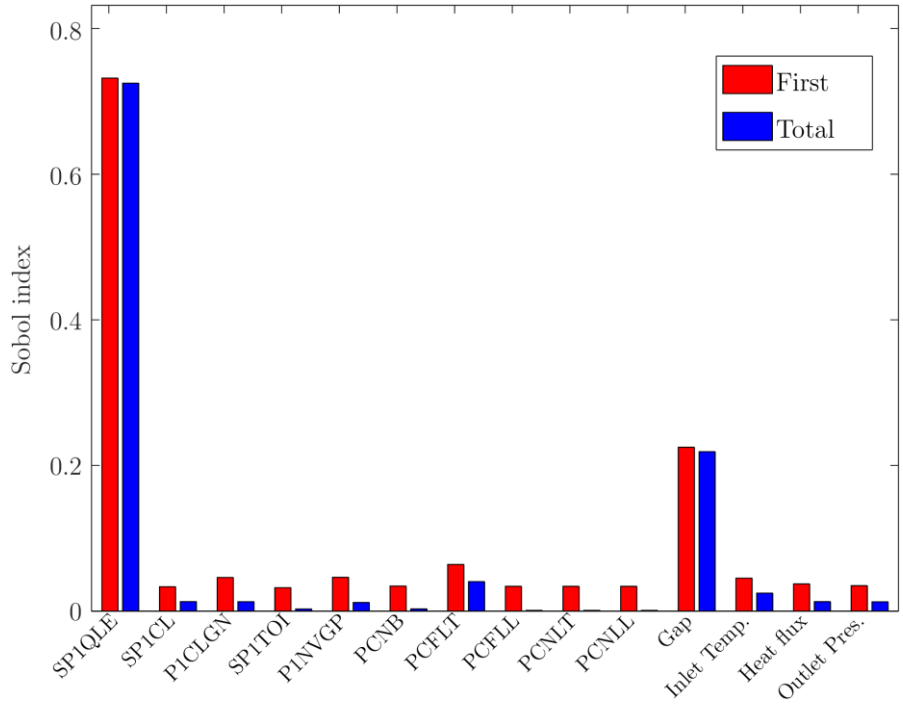

Figure 6. Sobol sensitivity indexes.

Table 5. Sobol sensitivity indexes.

	1st order			Total		
	Index	***Interval 95% - 95%***		***Index***	***Interval 95% - 95%***	
SP1QLE	0.732	0.702	0.760	0.725	0.668	0.783
SP1CL	0.034	0.000	0.095	0.013	0.012	0.015
P1CLGN	0.046	0.000	0.108	0.013	0.011	0.015
SP1TOI	0.032	0.000	0.094	0.003	0.003	0.003
P1NVGP	0.046	0.000	0.108	0.012	0.010	0.013
PCNB	0.034	0.000	0.096	0.003	0.003	0.003
PCFLT	0.064	0.002	0.126	0.041	0.036	0.046
PCFLL	0.034	0.000	0.096	0.001	0.001	0.001
PCNLT	0.034	0.000	0.096	0.001	0.001	0.001
PCNLL	0.034	0.000	0.096	0.001	0.001	0.001
Gap	0.225	0.165	0.283	0.219	0.196	0.244
T_{in}	0.045	0.000	0.107	0.025	0.022	0.028
ϕ	0.037	0.000	0.099	0.013	0.012	0.015
p_{out}	0.035	0.000	0.097	0.013	0.011	0.015

6. CONCLUSIONS

This paper presents an uncertainty and sensitivity analysis of a flow excursion experiment simulated with the best-estimate thermal-hydraulic code CATHARE. The flow excursion instability is a key safety

phenomenon in research reactors. A Whittle-Forgan experiment is analyzed. It was performed in a uniformly heated vertical narrow rectangular channel with gap size of 3.23 mm, upward flow and at low pressure. The flow excursion instability was experimentally determined by reducing the mass flux to the channel until the minimum of the S-curve was obtained, while maintaining all other parameters constant. This experimental transient is simulated with CATHARE and a good agreement is found.

After identification and quantification of the uncertain input parameters, a propagation of uncertainties is carried out with the statistical platform URANIE. The 95 % / 95 % tolerance interval of the output quantity of interest, i.e. the mass flux at the minimum of the flow redistribution curve, is determined using the Wilks formula. A total number of 336 simulations is performed. The obtained tolerance interval is relatively large (relative variations compared to the BE flow-rate between approximately -20 % and +30 %) indicating a significant impact of the input uncertainties on the flow excursion prediction in CATHARE.

The most influential input uncertainties are then determined via the sensitivity analysis. Using the simulations from the uncertainty propagation, the Pearson and Spearman correlation coefficients are computed. The mass flux at the onset of flow instability is mainly influenced by the uncertainty on the sub-cooled condensation model (Pearson and Spearman coefficients of -0.8). A significant impact is also associated to the uncertainty on the gap size (coefficients equal to -0.4). The observed correlations are negative and linear. These results are compared to the ones obtained with the Sobol methodology, which gives a more reliable and complete sensitivity analysis, but more expensive in terms of number of simulations (16000). Similar and consistent outcomes are obtained. The sub-cooled condensation model and the gap size explain respectively 73 % and 22 % of the output variance, while the other parameters are negligible. A linear dependence is observed between the subcooled condensation model, the gap size and the onset of flow instability.

NOMENCLATURE

A	m^2	Flow area	$\dot{m}$	kg/s	Mass flow rate
D_{heat}	m	Heated diameter $D_{heat} = \frac{4A}{P_{heat}}$	p	Pa	Pressure
D_{hydr}	m	Hydraulic diameter $D_{hydr} = \frac{4A}{P_{wet}}$	P_{wet}	m	Wetted perimeter
G	kg/m^2/s	Mass flux $G = \frac{\dot{m}}{A}$	P_{heat}	m	Heated perimeter
l_{heat}	m	Heated width	T	°C	Temperature
L_{heat}	m	Heated channel length	ϕ	W/m^2	Heat flux
$_{in}$		Inlet of the channel	$_{out}$		Outlet of the channel

ACKNOWLEDGMENTS

The current research project was conducted within a collaboration agreement TechnicAtome / CEA – Direction des Energies. The CATHARE code is developed in the framework of the NEPTUNE project, financially supported by CEA (Commissariat à l'Energie Atomique et aux Energies Alternatives), EDF, IRSN (Institut de Radioprotection et de Sûreté Nucléaire) and FRAMATOME. In this study, the simulations were performed with a version of CATHARE adapted and validated for research reactors that is co-developed with TechnicAtome.

REFERENCES

[1] M. Ledinegg, "Instability of flow during natural and forced circulation", *Die Wärme*, 61, 891-898 (1938).

[2] J. A. Boure, A. E. Bergles, L. S. Tong, "Review of two-phase flow instability", *Nuclear Engineering and Design*, 25, 165-192 (1973).

[3] G. Geffraye, O. Antoni, D. Kadri, G. Lavialle, B. Rameau, A. Ruby, "CATHARE 2 V2.5_2: A single version for various applications", *Nuclear Engineering and Design*, 241, 4456–4463 (2011).

[4] A. Ghione, F. Cochemé, "Qualification of the system code CATHARE for nuclear research reactors", *12th International Topical Meeting on Nuclear Reactor Thermal-Hydraulics, Operation and Safety (NUTHOS12)*, Qingdao, China, October 14-18 (2018).

[5] A. Ghione, B. Noel, P. Vinai, C. Demazière, "Assessment of thermal-hydraulic correlations for narrow rectangular channels with high heat flux and coolant velocity", *International Journal of Heat and Mass Transfer*, 99, 344-356 (2016).

[6] A. Ghione, B. Noel, P. Vinai, C. Demazière, "Criteria for onset of flow instability in heated vertical narrow rectangular channels at low pressure: an assessment study", *International Journal of Heat and Mass Transfer*, 105, 464-478 (2017).

[7] A. Ghione, B. Noel, P. Vinai, C. Demazière, "Uncertainty and sensitivity analysis for the simulation of a station blackout scenario in the Jules Horowitz Reactor", *Annals of nuclear energy*, 104, 28-41 (2017).

[8] R. H. Whittle, R. Forgan, "A correlation for the minima in the pressure drop versus flow-rate curves for sub-cooled water flowing in narrow heated channels", *Nuclear engineering and design*, 6, 89-99 (1967).

[9] J-B. Blanchard et al., "The Uranie platform: an open-source software for optimisation, meta-modelling and uncertainty analysis", *EPJ Nuclear Sciences & Technologies*, 5 (2019).

[10] H. Glaeser, "GRS method for uncertainty and sensitivity evaluation of code results and applications", *Science and Technology of Nuclear Installations*, 2008, 1-7 (2008).

[11] S. S. Wilks, "Determination of sample sizes for setting tolerance limits", *The Annals of Mathematical Statistics*, 12, 91-96 (1941).

[12] H. Glaeser, P. Bazin, J. Baccou, E. Chojnacki, S. Destercke, "BEMUSE phase VI report: Status report of the area, classification of the methods, conclusions and recommendations", *Technical report OECD NEA/CSNI/R(2011)4*, (2011).

[13] R. A. Fisher, *Statistical methods for research workers*, Oliver and Boyd (1958).

[14] M. F. Triola, *Elementary statistics*, Pearson (2006).

[15] J. C. Helton, J. D. Johnson, C. J. Sallaberry, C. B. Storlie, "Survey of sampling-based methods for uncertainty and sensitivity analysis", *Reliability Engineering and System Safety*, 91, 1175-1209 (2006).

[16] I. M. Sobol, "Sensitivity estimates for non-linear mahematical model," *Mathematical Modeling and Computational Experiment*, 1, 407-414 (1993).

[17] T. Homma, A. Saltelli, "Importance measures in global sensitivity analysis of non linear models", *Reliability engineering and system safety*, 52, 1-17 (1996).

[18] J.-M. Martinez, "Analyse de sensibilité globale par decomposition de la variance," *Meeting of GdR Ondes and GdR MASCOT-NUM*, Paris, France (2011).

[19] T. Wickett et al., "Report of the uncertainty methods study for advanced best-estimate code applications", *Technical report OECD NEA/CSNI 97*, vol. 2 (1998).

[20] A. De Crecy et al., "Uncertainty and sensitivity analysis of the LOFT L2.5 test: Results of the BEMUSE program", *Nuclear Engineering and Design*, 238, 3561-3578 (2008).

[21] M. Courtaud, K. Schleisiek, G. Coulon, F. Mazzili, “Compte rendu d’essais. Pertes de charge et redistribution de débit sur des canaux rectangulaires de 1.8 mm d’entrefer (type R.H.F.)”, *Technical report TT/67-7-B/MC-KS-GC-FM*, CEA, Grenoble, France (1967).

[22] P. Vernier, “Détermination expérimentale des courbes en S et des conditions de redistribution de débit”, *Technical report TT/65-19-B/PV*, CEA, Grenoble, France (1965).